

## ***Supplementary materials and methods***

### ***EIA assay for apelin***

$3 \times 10^4$  HUVECs were cultured in 48-well plates for 12hrs in Humedia EG2 (Kurabo Osaka, Japan). Cells were then incubated in M199 medium supplemented with 0.5% FBS. After 4hrs of serum deprivation, cells were incubated with basal medium containing 100-500 ng/ml of Ang-1 (R&D Systems, Minneapolis, MN). After stimulation for 24hrs, the concentration of apelin in the cell culture supernatants was evaluated using an apelin-12 EIA kit (Phoenix Pharmaceuticals Inc, Burlingame, CA) according to the manufacturer's instructions.

### ***RT-PCR analysis***

Total RNA was extracted from cells and tissues using the RNeasy plus mini kit (QIAGEN, Hilden, Germany) according to the manufacturer's protocol. Total RNA was reversed transcribed into cDNA using Exscript RT Reagent Kit (Takara, Otsu, Japan). Primer pairs for studying expression of mouse apelin, APJ, claudin5, VE-cadherin, CD31, occluding, and GAPDH by real-time RT-PCR and PCR are listed in Supplemental Table 1. Real-time PCR analysis was performed by Platinum SYBR Green qPCR SuperMix-UDG (Invitrogen). The levels of PCR products were monitored with an ABI PRISM 7900HT sequence detection system and analyzed with ABI PRISM 7900 SDS software (Applied Biosystems, Foster City, CA). The adjustment of baseline and threshold was performed according to the manufacturer's instructions. The relative abundance of transcripts was normalized to the constitutive expression level of GAPDH RNA.

### ***Western blotting***

Immunoblotting was performed to detect Tie2 phosphorylation and expression of claudin5,

VE-cadherin, CD31, and occludin in HUVECs. Total cell lysates (2  $\mu$ g total protein) were heated for 2 min at 95°C and then loaded onto SDS-polyacrylamide gels. Proteins were electrophoretically transferred onto polyvinylidene difluoride membranes, blocked with 5% nonfat dry milk, and subsequently incubated with anti-phospho-Tie2, -Tie2 Ab (Cell Signaling), -claudin5 (Zymed Laboratories, South San Francisco, CA), -VE-cadherin (R&D Systems), -CD31 (Pharmingen), or -GAPDH Abs (CHEMICON, Temecula, CA) according to the manufacturer's protocol. Proteins were detected with horseradish peroxidase conjugated anti-mouse, anti-rabbit (DAKO), or anti-rat secondary Ab (Biosource, Camarillo, CA) and ECL reagents (Amersham, Piscataway, NJ). Similarly, total cell lysates (2  $\mu$ g total protein) from OP9/vector or OP9/apelin were analyzed for the expression of apelin using anti-apelin mAb. Cell surface APJ expression of HUVECs was analyzed using a membrane protein fraction. Cell surface protein was collected using the modified biotinylation method with Qproteome Plasma Membrane Protein Kit (QIAGEN, Hilden, Germany) according to the manufacturer's protocol. Collected samples were then subjected to SDS-PAGE followed by immunoblotting with antibody against APJ, claudin5 (Zymed Laboratories) and GAPDH (Chemicon). Proteins were detected with horseradish peroxidase conjugated anti-rabbit and anti-mouse secondary Ab (Dako) and ECL reagents (Amersham Biosciences). In all experiments, the blots were scanned with an imaging densitometer LAS-3000 mini (Fujifilm, Tokyo, Japan). Predetermined molecular weight standards were used as markers. Protein concentration was measured by the protein assay dye reagent (BioRad, Hercules, CA) with BSA as a standard.

### ***Cord formation assay of HUVECs***

HUVECs were cultured for 20hrs in M199 medium with 10ng/ml VEGF and 0.5% FBS. Cells were then harvested and cultured for 10hrs in 24-well plates coated with Matrigel (BD

Bioscience, San Jose, CA) in the presence or absence of 100ng/ml of apelin (Bachem AG, Bubendorf Switzerland), anti-VE-cadherin blocking antibody (Bender MedSystems, Burlingame, CA), or control anti-B220 mAb.

### *Spheroid assay of HUVECs*

The preparation of EC spheroids was performed as described previously (Korff T. & Augustin H.G. J. Cell. Biol. 143: 1341-1352, 1998). Briefly, HUVECs stimulated with 10ng/ml VEGF for 24hrs were harvested and suspended in M199 medium supplemented with 1% FBS and 20% (w/v) carboxymethylcellulose (Sigma, St. Louis, MO).  $2 \times 10^5$  cells per dish were seeded into nonadhesive 35mm dishes (Falcon, Franklin lakes, NJ) for 10hrs at 37 °C. The size of the EC spheroid generated was measured and analyzed statistically.

## **Supplementary Figure legends.**

### **Figure 1. Apelin and APJ expression on HUVECs stimulated with various angiogenic cytokines**

4×10<sup>6</sup> HUVECs were cultured in 6-well culture plates for 12hrs in Humedia EG2. Cells were then incubated in M199 medium supplemented with 1% FBS. After 3hrs of serum deprivation, cells were incubated with basal medium containing 500ng/ml of Ang1, 10 or 30ng/ml of EGF, 10 or 30ng/ml of bFGF, 10 or 30ng/ml of PDGF-BB (R&D Systems, Minneapolis, MN), 20ng/ml of VEGF (PeproTech EC Ltd, Rocky Hill, NJ), or 100ng/ml of apelin (Bachem AG, Bubendorf Switzerland). Total RNA was extracted from cells grown under each culture condition and real-time PCR analysis was performed. Results are shown as fold-increase in comparison with basal levels of HUVECs.

(A) Apelin expression stimulated with VEGF. HUVECs were stimulated with VEGF for 0-22hrs. VEGF did not induce apelin expression in HUVECs. (B) Apelin expression stimulated with Ang1 as a positive control, EGF, bFGF, or PDGF-BB for 20hrs. \**P*<0.001 (n=3). Among the proangiogenic cytokines tested, bFGF as well as Ang1 significantly induced apelin expression. (C) APJ expression stimulated with Ang1. HUVECs were stimulated with Ang1 for 0-20hrs. Ang1 did not induce APJ expression. (D) APJ expression stimulated with EGF, bFGF, or PDGF-BB for 20hrs. These cytokines did not induce APJ expression in HUVECs.

### **Figure 2. Cell surface expression of APJ on HUVECs stimulated with VEGF**

HUVECs stimulated with (B) or without (A) VEGF (20ng/ml) for 24hrs were stained with anti-APJ Ab (green) and PI (red) as described in Material and Methods of the main text. Stained samples were analyzed by confocal laser scanning microscopy (LSM510, Carl Zeiss,

Germany). Predominant membrane localization of APJ was observed in the presence of VEGF. Bottom picture represents the 3D reconstruction of z-stack (1  $\mu$ m xy slices indicated by white bar). Scale bar in (A) indicates 20  $\mu$ m.

**Figure 3. Comparison of the proliferation of ECs from different tissues responsive to apelin**

The heart and liver were dissected from 8-week-old adult ICR mice, and the AGM region from E11.5 ICR embryos. Tissues were dissociated by collagenase type II treatment. CD31<sup>+</sup>CD45<sup>-</sup> vascular ECs were sorted by JSAN flow cytometer (Bay Bioscience, Kobe, Japan) from each type of tissue and then  $3 \times 10^3$  ECs were cultured on OP9/vector or OP9/apelin cells in 24-well culture plates. After 6 days of culturing, cells were harvested and analyzed by FACS Calibur (Becton Dickinson, Franklin Lakes, NJ). The % of ECs among the total number of cells was calculated and presented. There was no real difference in the total number of cells in each culture plate. \* $P < 0.001$  (n=3). Note that ECs located in the AGM region, but not in adult heart or liver, were highly responsive to apelin-induced proliferation.

**Figure 4. Endothelial sheet formation by apelin**

Cells from E11.5 AGM region were cocultured for 6 days with an OP9/vector, OP9/apelin in the presence of B220 control antibody, or OP9/apelin in the presence of anti-apelin blocking antibody. ECs on OP9 cells were stained with anti-CD31 (red) and anti-claudin5 (green; Abcam Inc, Cambridge, MA) antibodies. Merged images are presented in the right panel. The insets are high-power views. Scale bar indicates 100  $\mu$ m.

**Figure 5. Junctional protein induction by apelin**

(A) Quantitative real-time RT-PCR analysis for claudin5, VE-cadherin, CD31, and occludin

using total RNA from HUVECs stimulated with 100ng/ml of apelin for 0-22hrs. Results are shown as fold-increase expression in comparison with levels in 0hrs stimulated HUVECs. \* $P < 0.01$ , (n=3). (B) Western blot analysis for adhesion molecules (claudin5, VE-cadherin, CD31) was performed using cell lysate from HUVECs stimulated with apelin (100ng/ml) for 14hrs.

**Figure 6. Confocal laser scanning analysis of cord-like structure induced by apelin.**

HUVECs were cultured in the presence of VEGF (20ng/ml) for 20hrs, harvested, transferred onto Matrigel, and cultured in the absence (A) or presence of apelin (B) for 10hrs as described in Figure 5 of the main text. HUVECs were pre-labeled with green fluorescent cell linker dye by using PKH67 cell linker mini kit (Sigma). Nuclei were stained with PI (red) after fixation. Structural analysis was performed by using confocal laser scanning microscopy. Bottom pictures represent the 3D reconstruction of z-stack (1 $\mu$ m xy slices indicated by white bar). Quantitative evaluation of the diameter (width) of the cord-like structure was presented in Figure 5A,d of the main text. Scale bar indicates 20 $\mu$ m.

**Figure 7. APJ expression in head region at E9.5 embryo**

(A) Whole-mount immunohistochemistry of E9.5 embryos, using anti-CD31 mAb or anti-APJ antibody, was performed as described in the Materials and Methods. (B) Schematic representation of staining profiles as observed in (A). CD31 marks all of ECs including anterior cardinal vein (ACV). APJ expression was observed in ACV; however, it was not expressed on ECs in the base of ACV (part of bidirectional arrows), but was expressed on those in the migration end region, as observed in the intersomitic vessel (ISV) described in the main text.

### **Figure 8. Apelin expression in ISV at E9.5 embryo**

Whole-mount immunohistochemistry of E9.5 embryos using anti-apelin antibody (C,D). Non-specific immunoreaction of this staining was observed using secondary antibody alone (A,B). (B) and (D) show high-power views of the areas indicated by a box in (A) and (C), respectively. Note that apelin expression was observed in the intersomitic vessel (ISV) (D).

### **Figure 9. Generation of apelin-deficient mice**

A mouse apelin gene was isolated from mouse strain 129/SvJ genomic library by using mouse *Apln* cDNA fragment as a probe, and a positive clone was selected and subcloned into Bluescript SK+ (Stratagene, La Jolla, CA). For construction of the targeting vector, genes containing 5'-end upstream region (1kbp) and 3'-end downstream region (7kbp) of *apln* gene exon2 were inserted into pGT-N28 vector (New England Biolabs) between *HindIII-BamHI* site and *EcoRI-XhoI* site, respectively. Herpes simplex virus thymidine kinase gene was used as a negative selection marker and was inserted between the *XhoI-NotI* site to yield the final targeting vector (pmA10TG-tk). The RW-4 ES cells (Genome Systems, St. Louis, MO) were electroporated with linearized targeting vector using gene parser (BioRad), and selected with Geneticin and FIAU. Single clones were picked and expanded for screening and storage. Genomic DNA was extracted from the ES clones, PCR analysis was performed to amplify a 1,300-bp fragment using the primer set of 5'-GCAGTAAAAGTAGGAAACAAGGGGGTGATG-3' and the 5'-TTGTGGTTCTAAGTACTGTGGTTTCC-3' for mutant allele and for wt allele. To further confirm the PCR results, Southern blot analysis was also performed. Genomic DNA was digested with *NcoI*, and hybridized with an internal probe to detect the 3.8-kb targeted allele. Targeted clone was chosen for C57BL/6NCrj blastocyst injection and produced chimeric founders and yielded germ line transmission of the targeted *apln* allele. Chimera

males were mated with C57BL/6J females and the offspring screened by Southern blot and PCR analyses for mice bearing the *apln*-deficient genotype. Primers used for detection of WT or mutant allele were as follows; sense, 5'- GCAGGAGGAAATTTTCGCAGACAGC -3' and 5'- ACCGGCACCGGGAGGGCACTT-3'(wt;700bp), and sense, 5'- GCAGTAAAAGTAGGAAACAAGGGGGTGATG-3' and 5'- TTGTGGTTCTAAGTACTGTGGTTTCC -3' (apelin mutant; 1300bp).

(A) Graphic representation of *Apln* gene and targeting strategy. The entire exon 2 codes a mature apelin peptide and their flanking regions were replaced by a neo cassette by homologous recombination. Sites of PCR primers (arrowheads) and probe (thick line) used for genotyping are indicated. Restriction sites: B, *Bam*HI; E, *Eco*RI; H, *Hind*III; N, *Nco*I; X, *Xba*I. TK, thymidine kinase gene cassette. (B) Genotyping of apelin-mutant ES cells (left) and apelin-deficient mice (right). (left) Identification of the targeted allele by Southern blot analysis. Genomic DNA of ES clones were digested with *Nco*I and hybridized with probe located outside in 5' flanking region of exon 2. The targeted clone gave a band at 3.8 kb, while the original ES cells RW4 gave a band at 6.9 kb. (right) RT-PCR analysis of apelin-deficient mice. Apelin<sup>+/-</sup> mice have both the WT (1000bp) and mutant (700bp) bands.

**Figure 10. Calculation of diameter of intersomitic vessels from WT and apelin KO E9.5 embryos**

(A) Schematic representation of how tissue sections in (B) were obtained. The left panel shows whole views, and the right shows transverse views. Nos. 1~5 in these schematic diagrams correlate with the section number presented in (B). (B) Sections derived as presented in (A) were stained with anti-CD31 antibody. Panels 1~5 show serial sections derived from one E9.5 WT or apelin KO embryo. Diameter of the luminal cavity of the intersomitic vessel (ISV) was measured as a distance between two parallel red lines as



described in panel No.2. DA: dorsal aorta, a: anterior, p: posterior, r: right, l: left. Scale bar indicates 50  $\mu$ m.

**Figure 11. Comparison of number of blood vessels and lymphatic vessels observed in the skin from 8-week-old WT and apelin KO mice.**

Transverse sections of dermis from normal mice were stained with anti-CD31 and anti-LYVE1 mAb [specific antibody for lymphatic ECs; a gift from Dr. Oike, Keio University, Tokyo. (Morisada et al. (2005) *Blood* 102)]. Skin sections had higher autofluorescence and it was difficult to determine whether the overlapping signal was actually derived from a double positive signal or not. Therefore, in this assay, we stained one section chemically by two steps, as follows. Firstly, one section was stained with anti-CD31 mAb followed by ALP conjugated goat-anti-Rat Igs (Biosource) and New Fuchsin (DAKO) as a substrate for obtaining a red color reaction. Then after extensive washing, the same section was stained with biotinylated anti-LYVE-1 mAb followed by HRP-conjugated streptavidin ABC complex (DAKO) and DAB (Dojindo, Kumamoto, Japan) as a substrate for obtaining a dark blue reaction. We counted the number of vessels by dividing the skin into the dermis and the hypodermis. Blood vessels were characterized as CD31<sup>+</sup>LYVE-1<sup>-</sup> and lymphatic vessels as LYVE-1<sup>+</sup>. In the hypodermis, there were very few lymphatic vessels, so we could not evaluate the number of hypodermic lymphatic vessels. Vessels were divided into three groups based on their caliber size as described. Data clearly showed that blood vessels observed in apelin KO mice were narrower compared to those in WT mice, in both the dermis and hypodermis. There were no significant differences in the caliber size of the lymphatic vessels between WT and apelin KO mice. Data shown are representative samples from one mouse selected from three independent WT or apelin KO mice. 50 random fields were examined.

**Figure 12. Blood vessel formation in the yolk sac from E8.5 and E9.5 WT and apelin KO embryos**

Whole-mount immunohistochemistry of the yolk sacs from E8.5 and E9.5 WT and apelin KO embryos was performed using anti-CD31 antibody. At E8.5, there was no difference between WT and apelin KO mice in the formation of blood vessels constructed by the vasculogenesis process. At E9.5, remodeling of blood vessels composed of large and small vessels was similarly observed in WT and apelin KO mice.

**Figure 13. Apelin and APJ expression on HUVECs affected by shear stress**

HUVECs were seeded in 6cm cell culture dish until confluence was reached and cells were then incubated in Hanks' Balanced medium (Sigma) for 6hrs. The shear stress experiments were performed with pulsatile flow (12-7dynes/cm<sup>2</sup>) as described previously (SenBanerjee et al., J. Exp. Med. 199: 1305-1315, 2004, Fledderus et al., Blood 109: 4249-4257, 2007), using a Viscomter controller RC-100 (Toki sangy, Japan). After the indicated treatments, either total RNA was obtained and analyzed by real-time quantitative PCR. For the detection of human APJ, human apelin, or KLF2 gene which has been reported to upregulate under shear stress (SenBanerjee et al., 2004, Fledderus et al., 2007), the following primers were used (human APJ: Sense 5'- CAC CAC GGG AAA CGG TCT G-3'; Antisense 5'- GGT ACG TGT AGG TAG CCC ACA-3', human apelin: Sense 5'- GTC TCC TCC ATA GAT TGG TCT GC -3'; Antisense 5'- GGA ATC ATC CAA ACT ACA GCC AG-3' , KLF2: Sense 5'-ACT CAC ACC TGC AGC TAC GC-3'; Antisense 5'-TGC AGT GGT AGG GCT TCT CA-3'). Results are shown as fold-increase expression in comparison with levels in non-stimulated HUVECs. \*P < 0.01.

## References

- SenBanerjee S, Lin Z, Atkins GB, Greif DM, Rao RM, Kumar A, Feinberg MW, Chen Z, Simon DI, Luscinskas FW, Michel TM, Gimbrone MA Jr, Garcia-Cardena G, Jain MK (2004) KLF2 Is a novel transcriptional regulator of endothelial proinflammatory activation. *J Exp Med* **199** : 1305-1315
- Fledderus JO, van Thienen JV, Boon RA, Dekker RJ, Rohlena J, Volger OL, Bijmens AP, Daemen MJ, Kuiper J, van Berkel TJ, Pannekoek H, Horrevoets AJ (2007) Prolonged shear stress and KLF2 suppress constitutive proinflammatory transcription through inhibition of ATF2. *Blood* **109** : 4249-4257.

### **Figure 14 Matrigel plug assay using apelin**

0.3ml of Matrigel (BD Bioscience, San Jose, CA ) containing the apelin (1000ng/ml) and/or VEGF (100ng/ml) were injected subcutaneously into C57BL/6 mice. After 7 days, the mice were injected intraperitoneally with BrdU reagent (100 $\mu$ g/g body weight). Three days after the BrdU injection, the mice were sacrificed and the Matrigel plug was dissected out, and homogenized. To quantify the proliferation of ECs in the Matrigel plug, BrdU-positive cells were measured using a BD Pharmingen BrdU Flow Kit (BD Pharmingen, San Jose, CA) following the manufacturer's protocol and CD31<sup>+</sup>, BrdU<sup>+</sup> cells were measured by FACS Calibur (Becton Dickinson, Franklin Lakes, NJ ). Three mice were used for each group, and the experiments were duplicated. Results indicated that 70% of ECs located in VEGF-containing Matrigel were BrdU<sup>+</sup> proliferating ECs. On the other hand, 40% of ECs in apelin-containing Matrigel expressed BrdU. Therefore, these results indicated that apelin alone induces angiogenesis by promoting EC migration by a chemoattractive manner rather than by inducing proliferation of ECs. Apelin has been reported to induce angiogenesis in the Matrigel plug assay (Kasai et al., *Biochem Biophys Res Commun.* 325:395-400, 2004) and to

induce the chemotaxis of ECs (Cox et al., Dev Biol 296: 177-189, 2006). Therefore, our data presented here are consistent with previous reports.

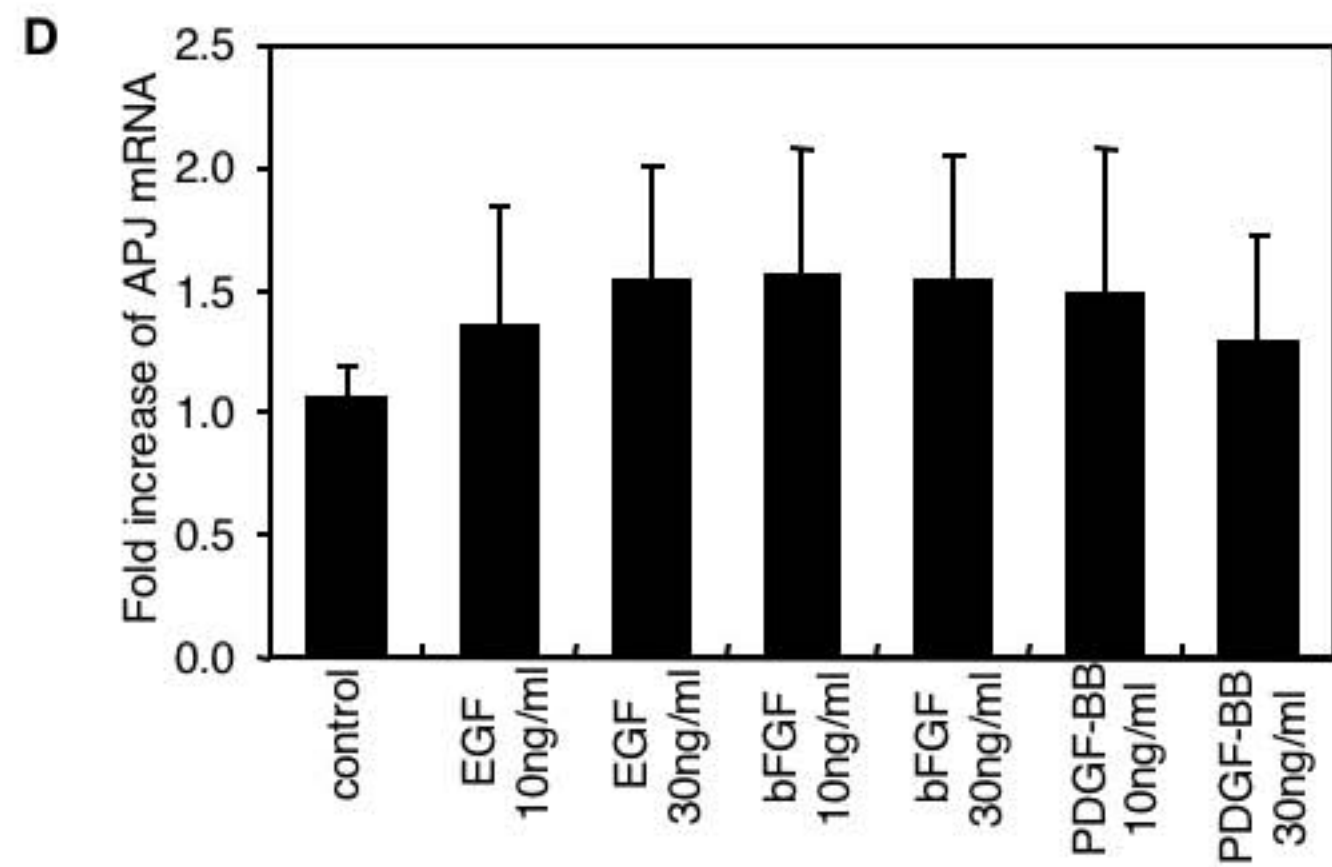
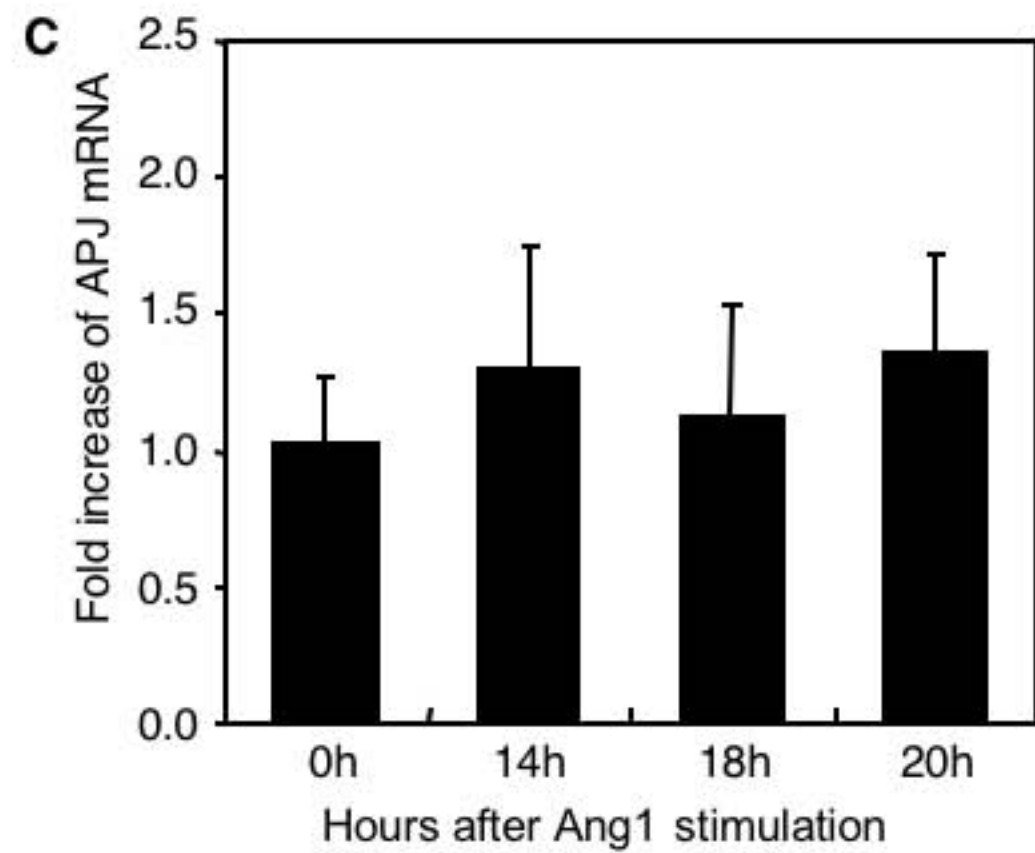
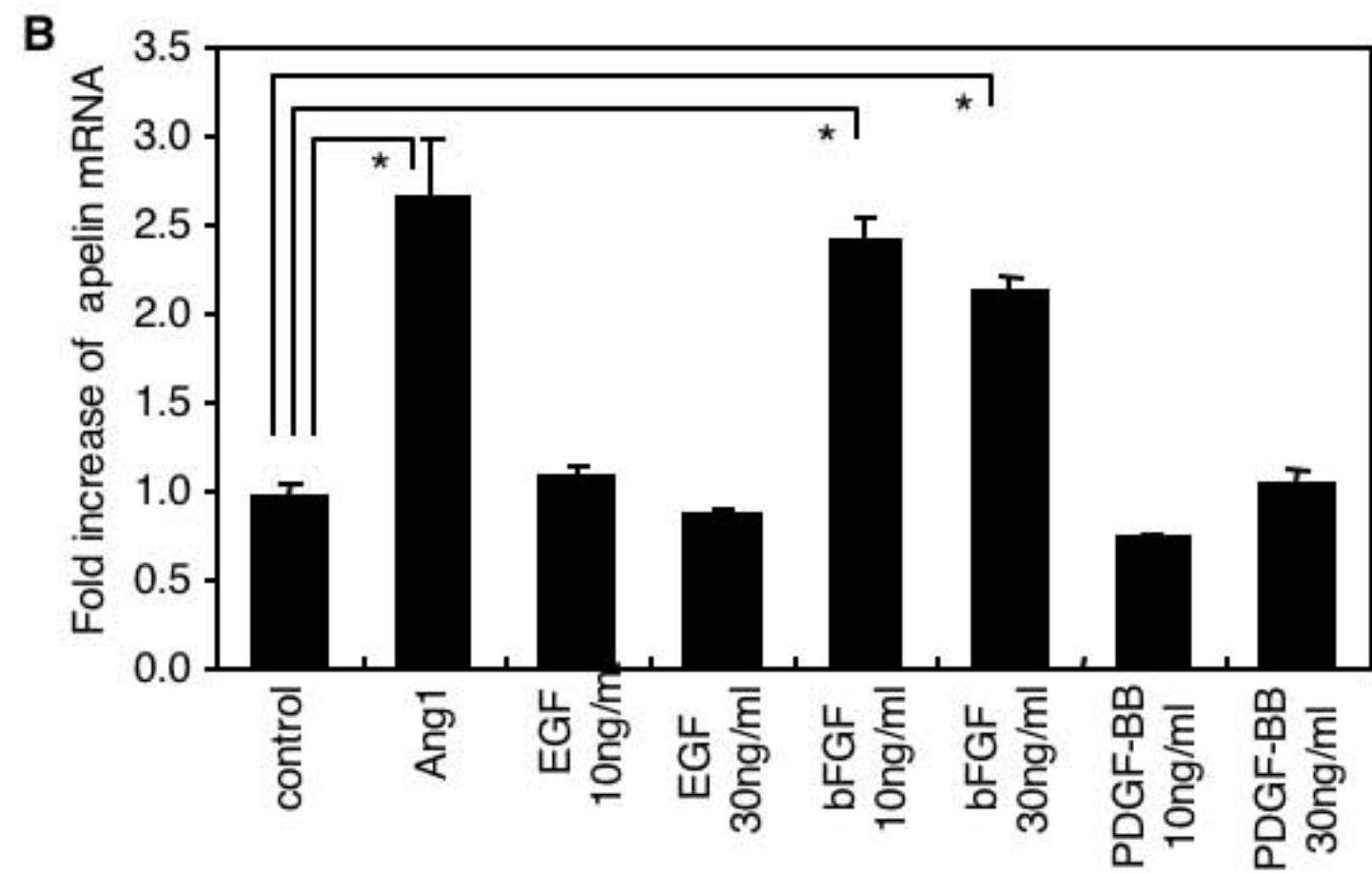
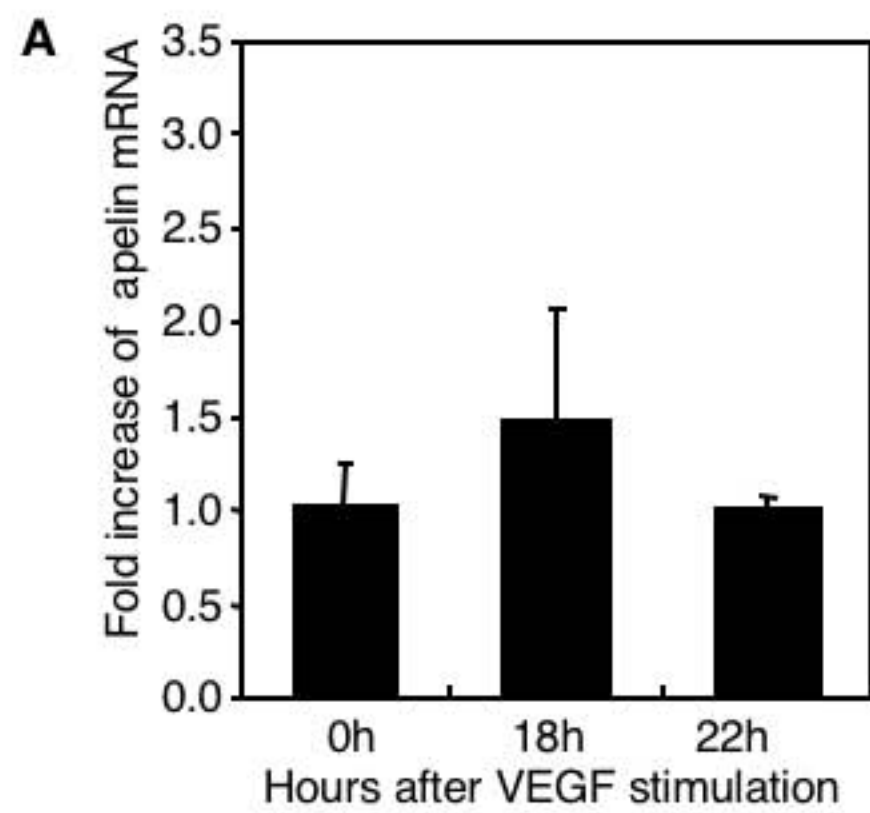
### **Figure 15 Modification of cytoskeleton structure by apelin**

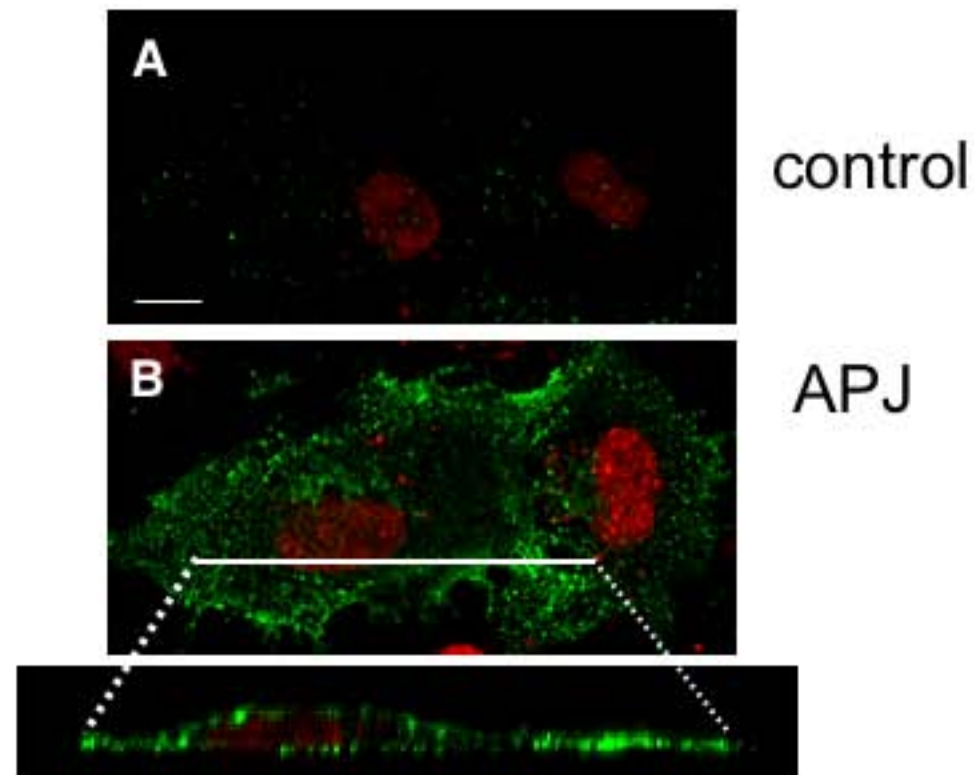
HUVECs were cultured in 35mm glass-bottomed dishes (IWAKI, Tokyo, Japan) overnight in Humedia EG2 (Kurabo). Cells were then incubated in M199 medium with 0.5% FCS. After 10hrs of serum deprivation, cells were incubated with basal medium containing 100ng/ml of Apelin or 20ng/ml of VEGF. Five minutes after stimulation, cells were fixed with 4% paraformaldehyde and permeabilized by Triton X100, and stained by TRITC-conjugated phalloidin (red) and Hoechst (blue; Sigma, St Louis, MO). Stained samples were analyzed by confocal laser scanning microscopy (LSM510, Carl Zeiss, Germany). The pictures on the bottom row are high-power views of the corresponding areas outlined by dashed lines, in the respective pictures on the top row. As observed following VEGF treatment, apelin induced stress fiber formation. Scale bar indicates 50 $\mu$ m.

### **Figure 16. Suppression of the inhibitory activity of apelin on cAMP production by anti-apelin mAb**

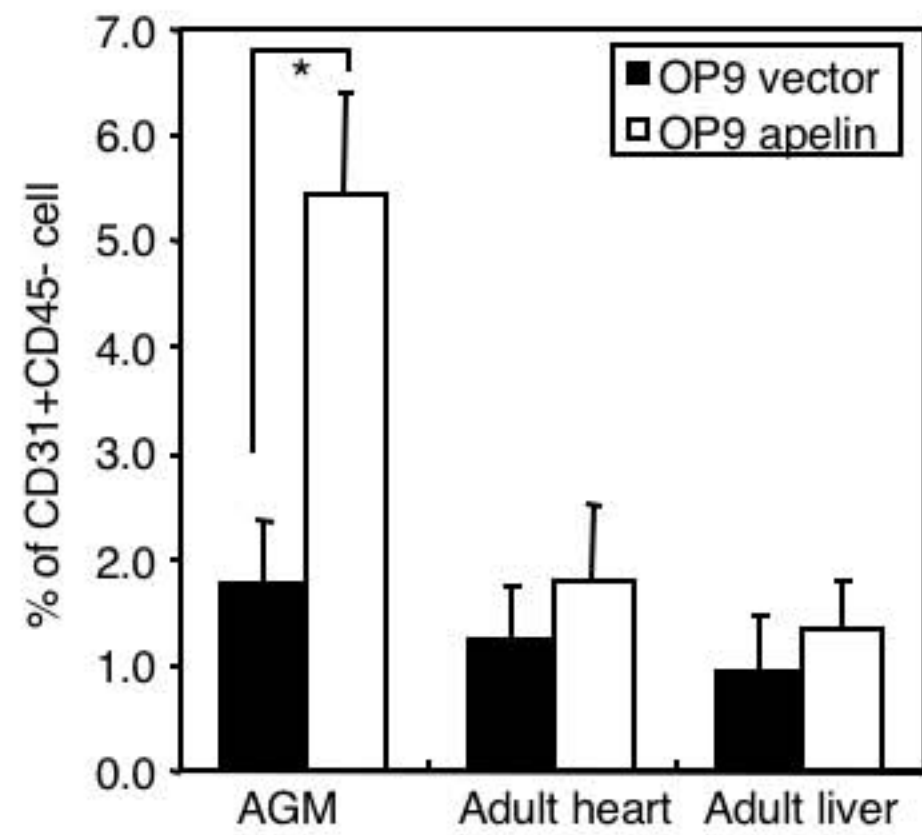
It has been reported that forskolin (FSK)-stimulated cAMP production in CHO cells expressing APJ was inhibited by the addition of apelin-13 (Habata Y. et al. Biochimica et Biophysica Acta 1452;25-35, 1999). We investigated whether anti-apelin monoclonal antibody (4G5) inhibits the suppressive effect of apelin on cAMP production from CHO cells expressing APJ. CHO cells, introduced with APJ cDNA (CHO/APJ) or mock vector (CHO/mock), were established as described previously (Tatemoto K. et al. Biochem. Biophys. Res. Commun. 251;471-476, 1998). The inhibitory activity of apelin (0.3nM) on cAMP production by these cells in the presence or absence of anti-apelin mAb (4G5) ranging from

0-10nM was measured in the presence of 0.2mM 3-isobutyl-1-methylxanthine (IBMX, Sigma, St. Louis, MO, USA) and 2 $\mu$ M FSK (Wako, Osaka, Japan) in an *in vitro* culture, and the amount of cAMP was determined with a cAMP enzyme immunoassay (EIA) system (Amersham, Buckinghamshire, UK) according to the manufacturer's instructions. (A) The amount of cAMP used by CHO/APJ cells (n=3). (B) The amount of cAMP used by CHO/mock cells (n=3). FSK-induced cAMP production from CHO/APJ cells inhibited by the addition of apelin-13. This inhibition was suppressed by anti-apelin mAb, in a dose-dependent manner, in CHO/APJ cells (A) but not in CHO/mock cells (B).



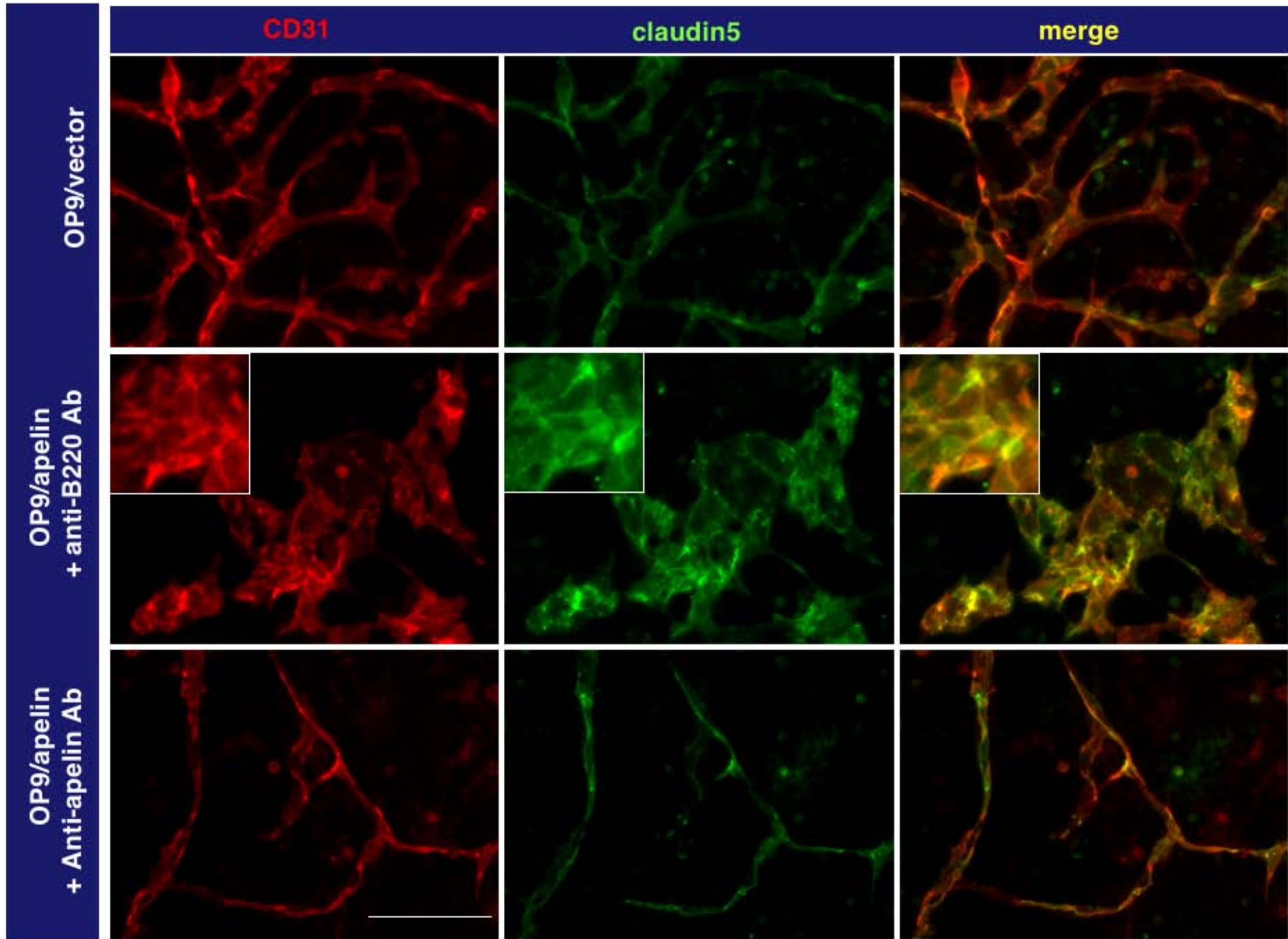


Supplemental Figure 2 Kidoya H. et al.

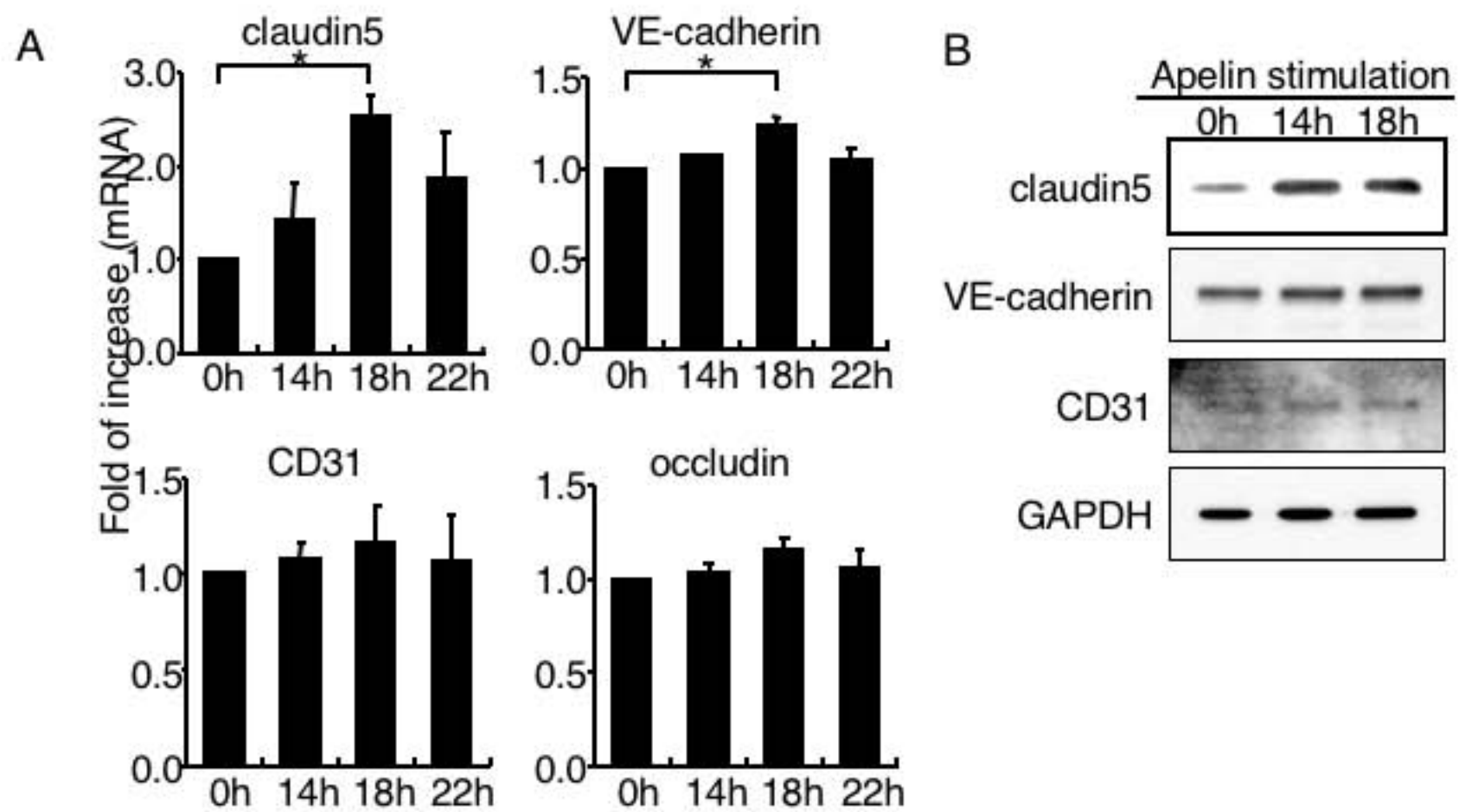


Supplementary Figure 3 Kidoya H. et al.

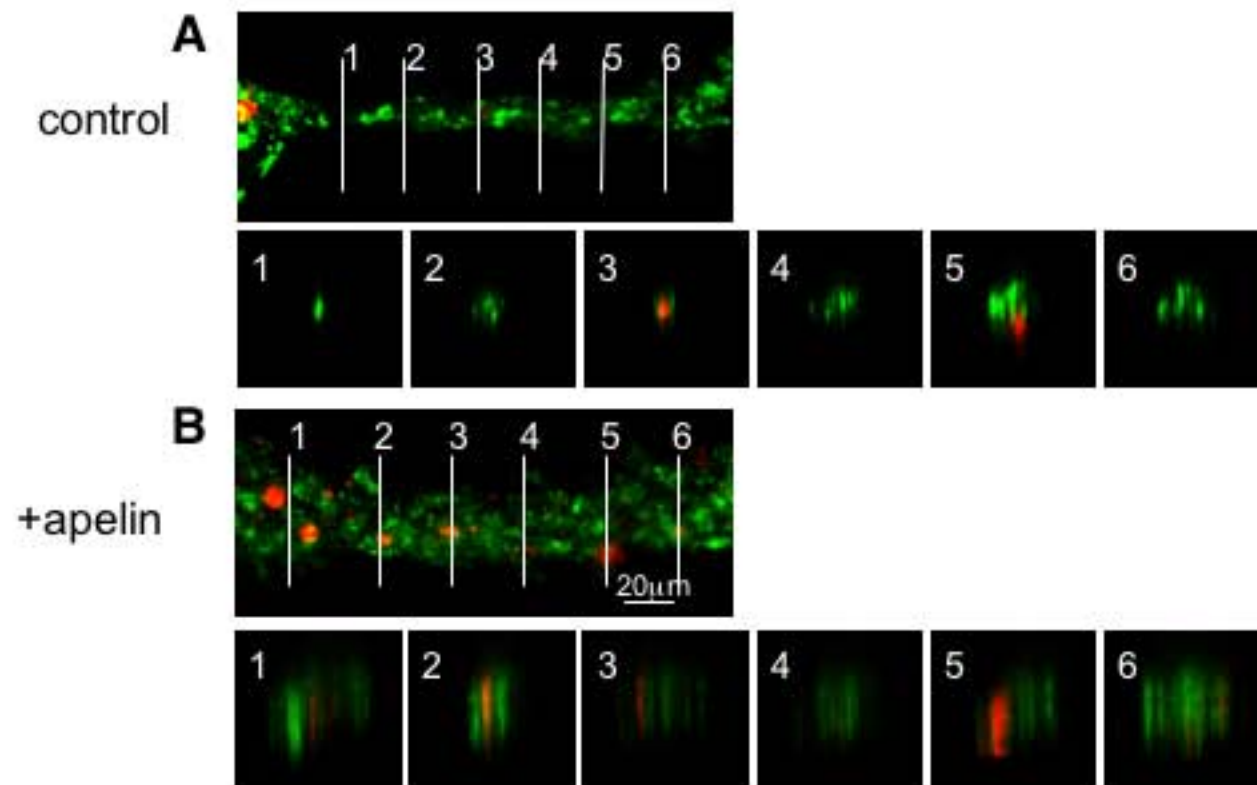




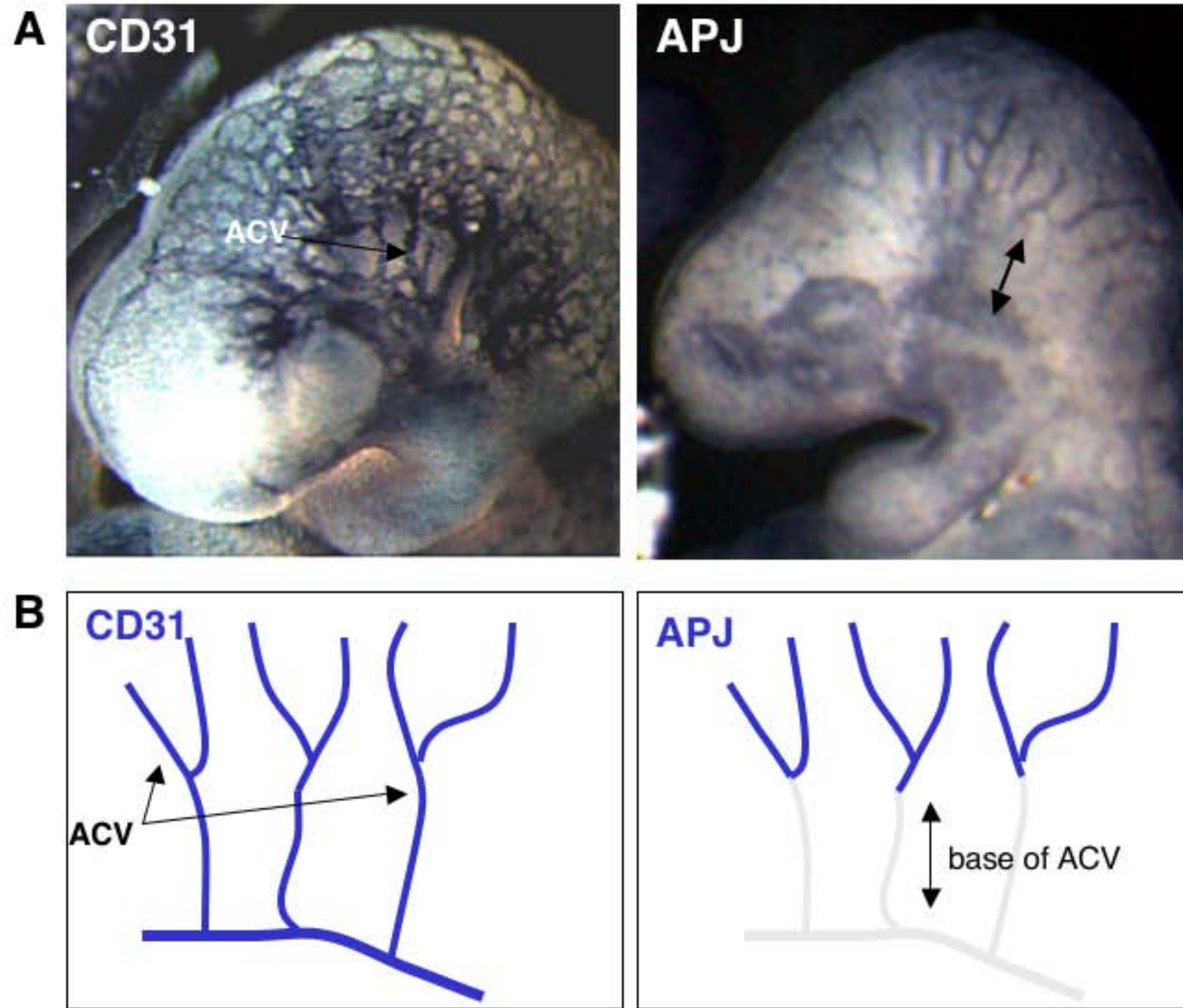
Supplementary Figure 4 Kidoya H. et al.



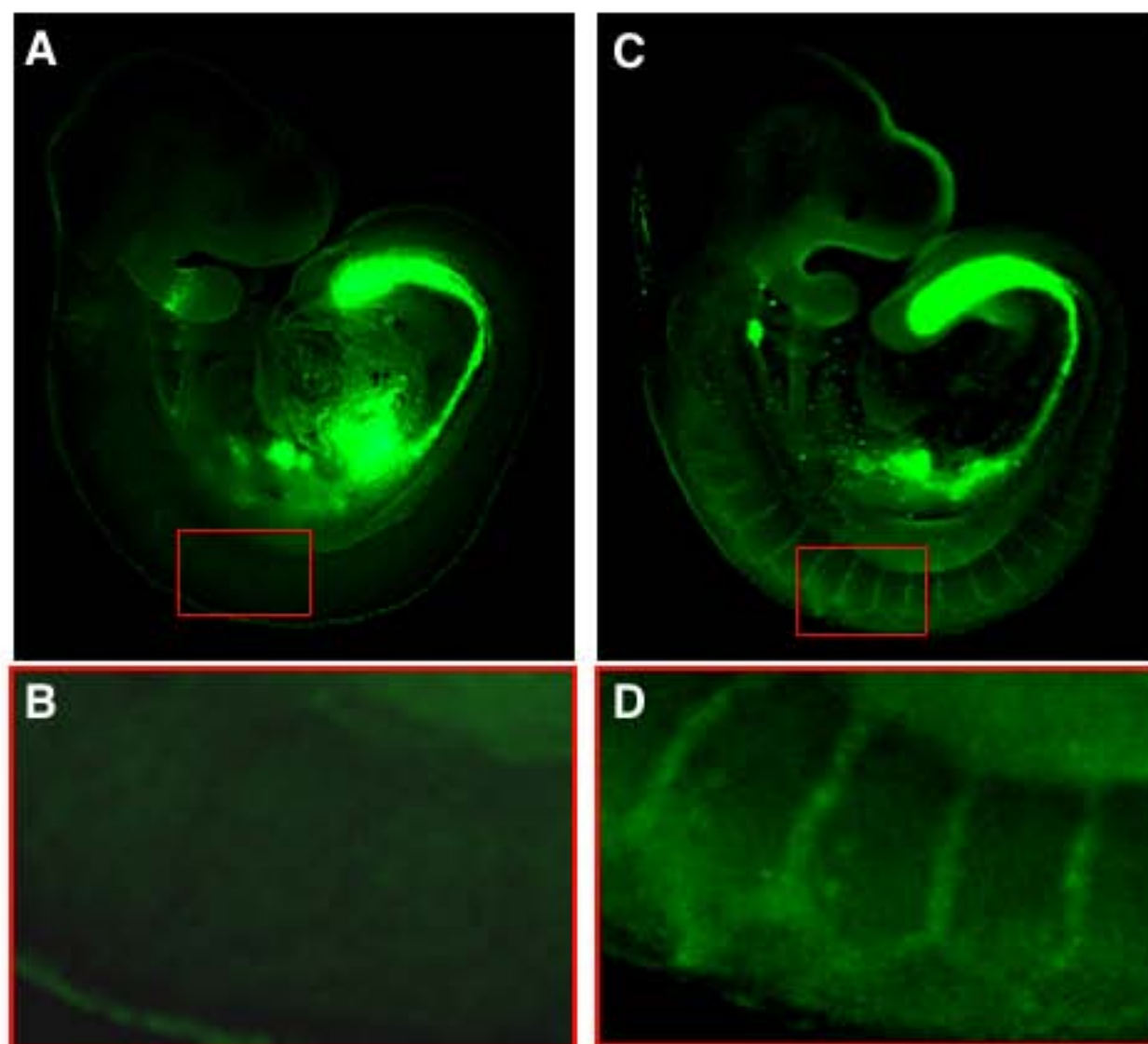
Supplementary Figure 5 Kidoya H. et al.



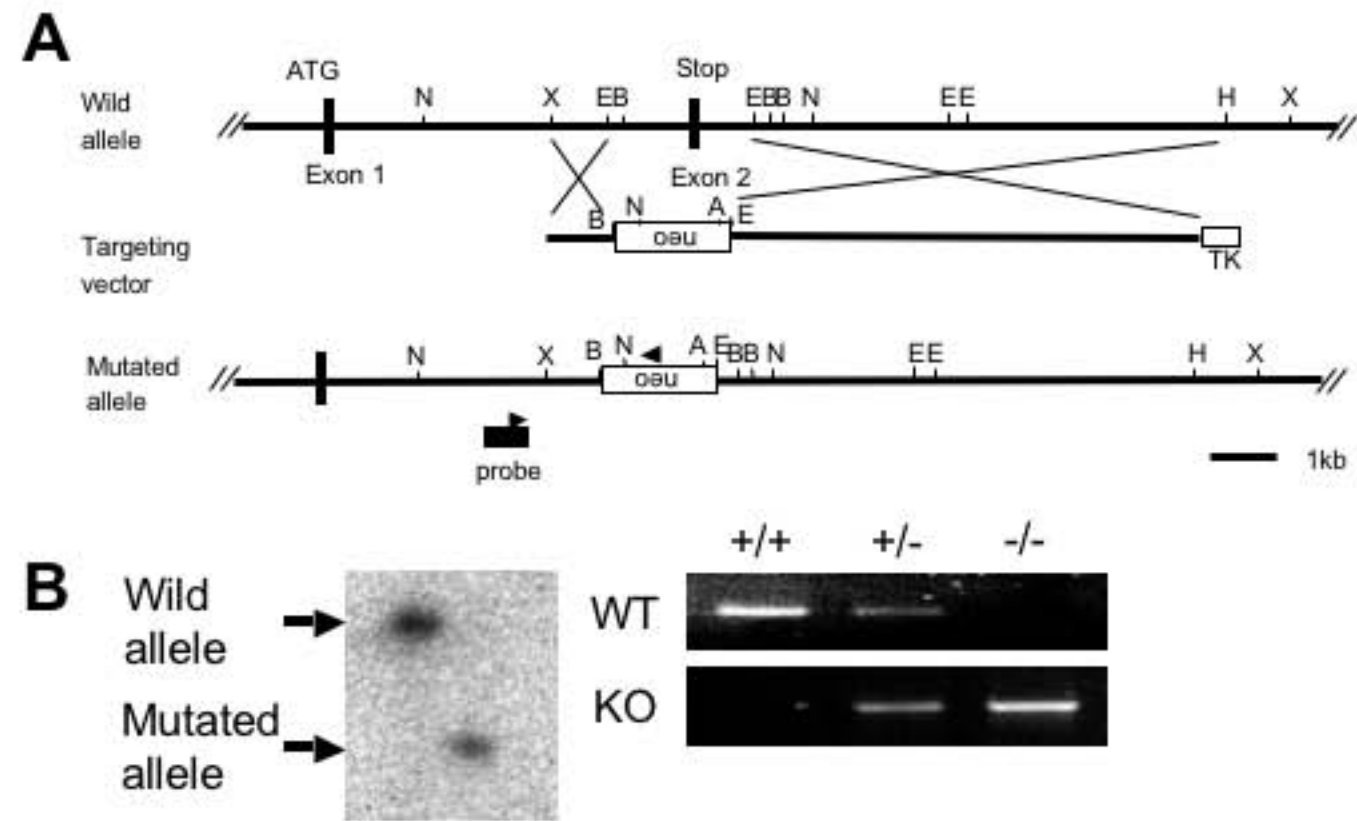
Supplementary Figure 6 Kidoya H. et al.



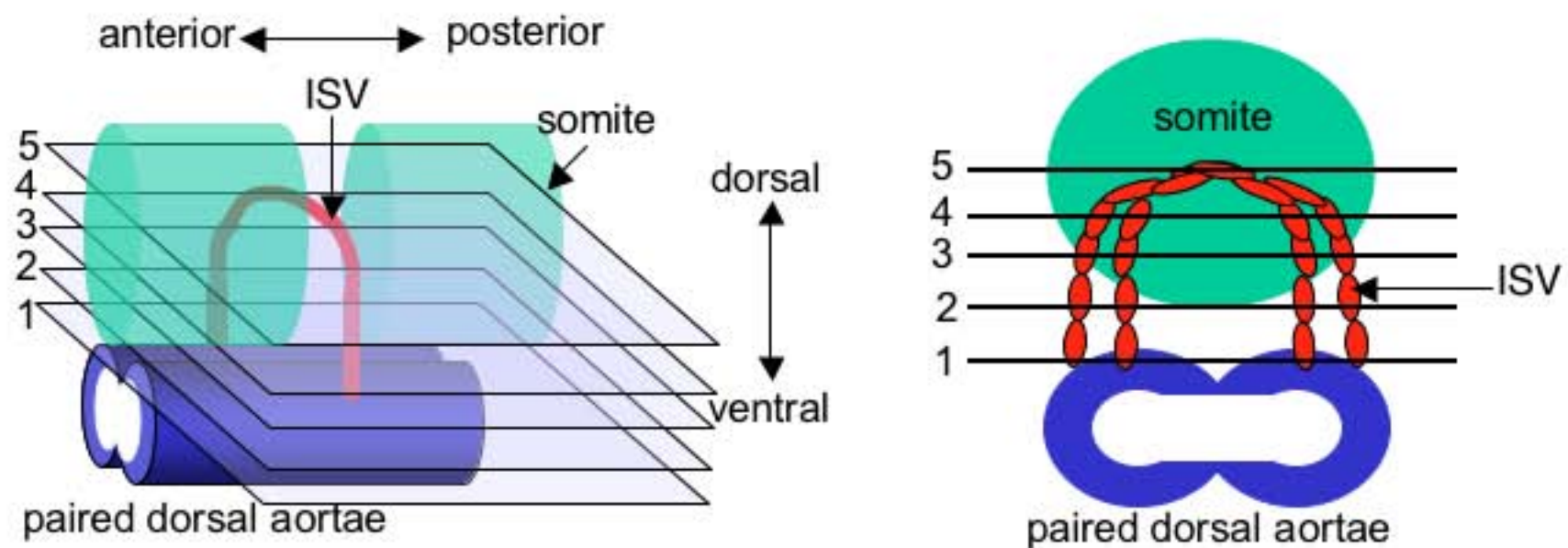
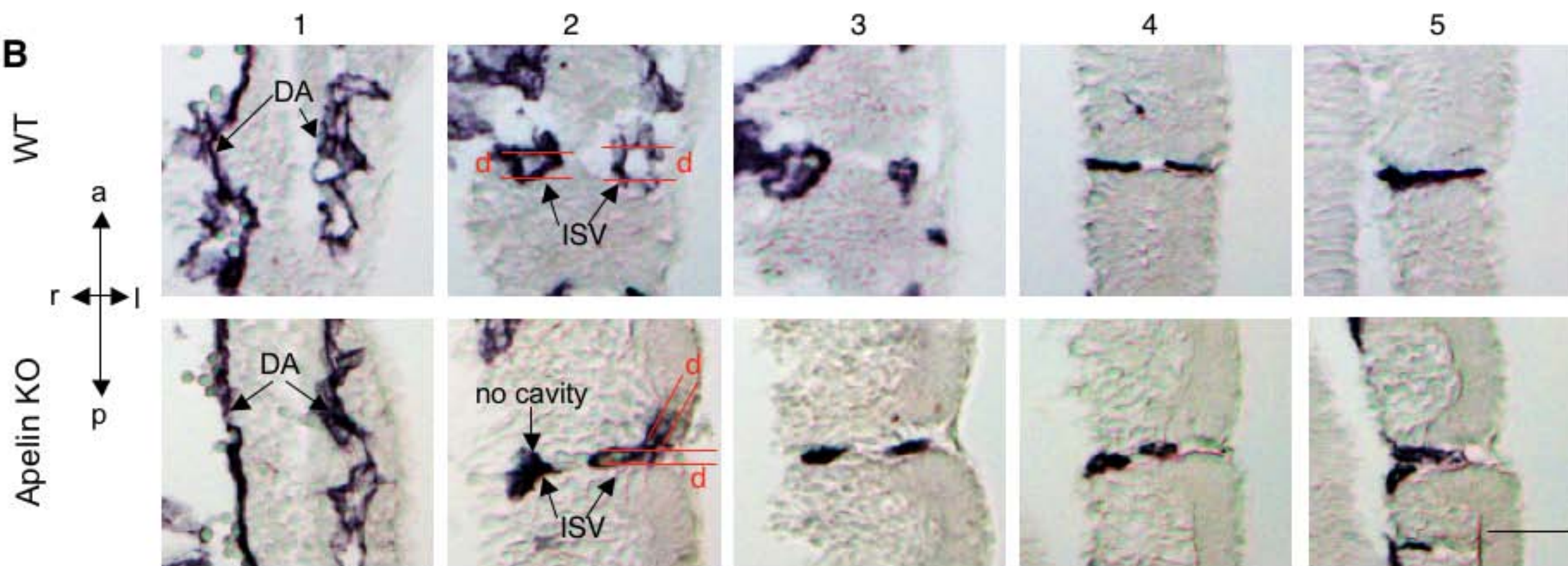
Supplementary Figure 7 Kidoya H. et al.

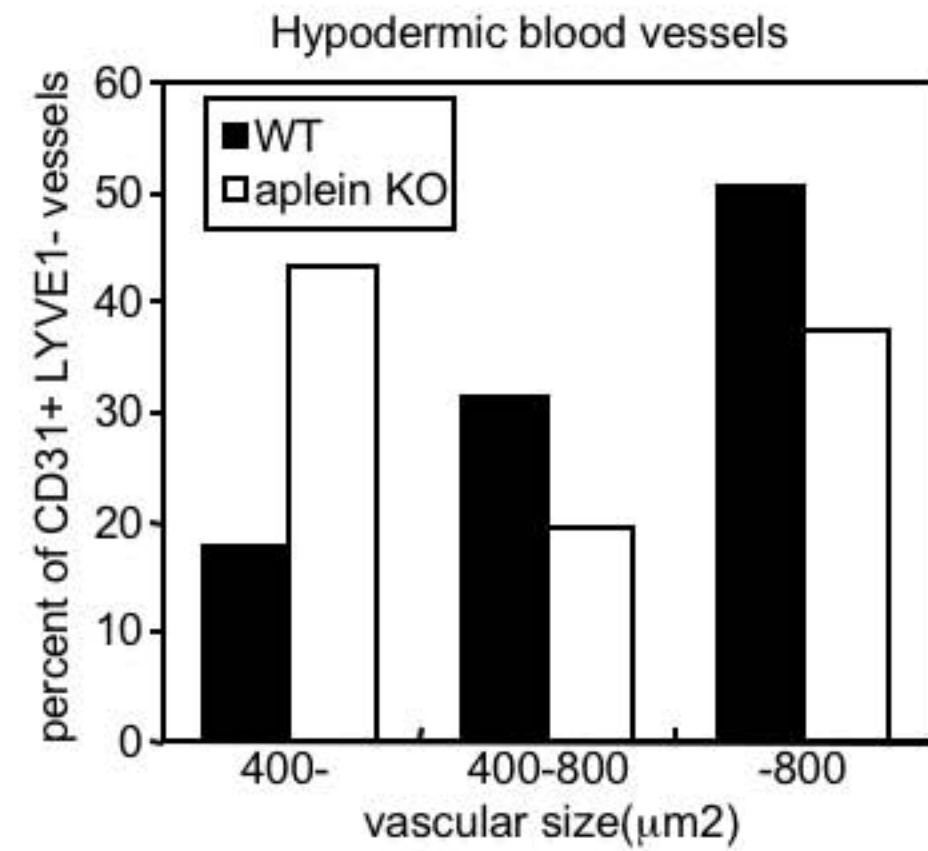
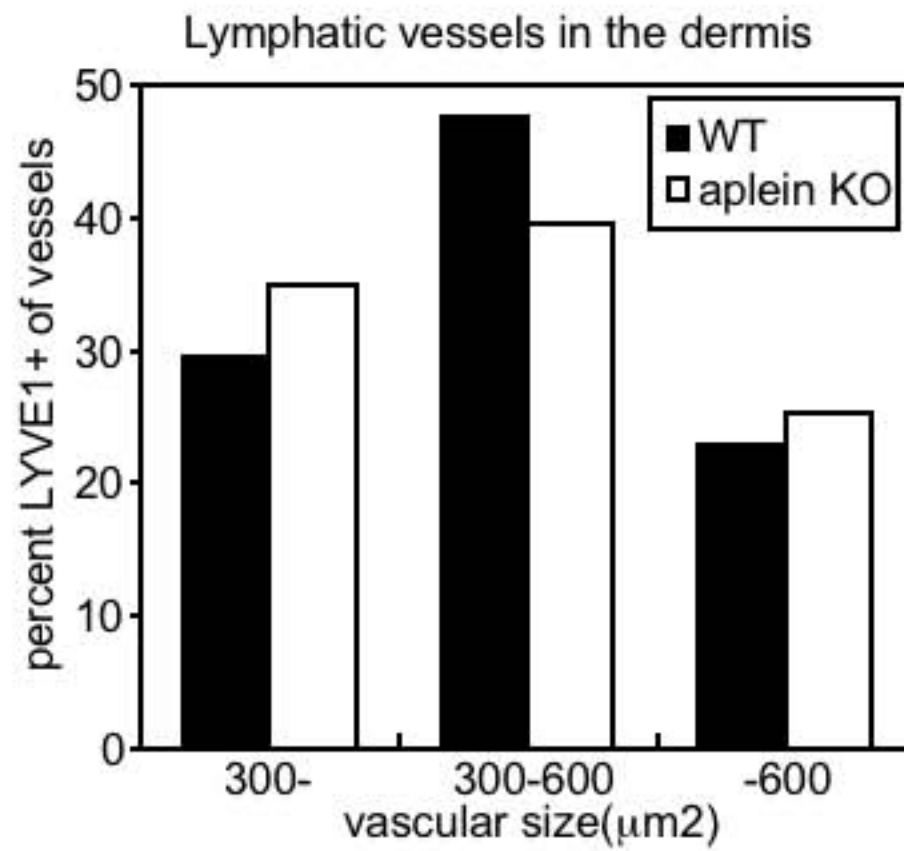
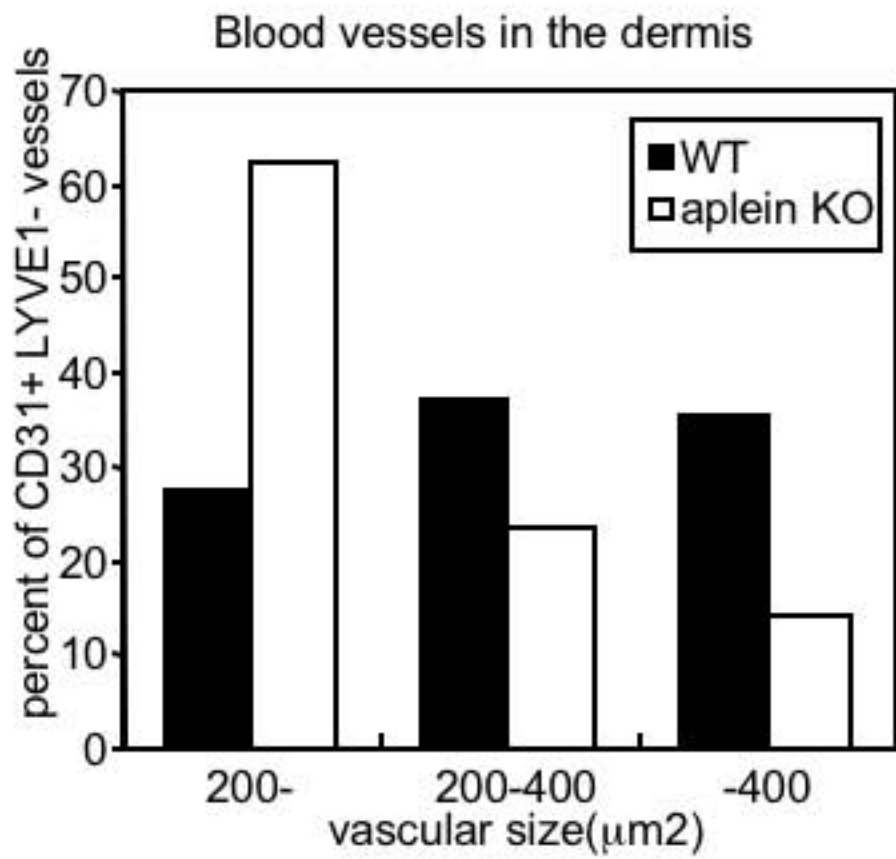


Supplementary Figure 8 Kidoya H. et al.



Supplementary Figure 9 Kidoya H. et al.

**A****B**

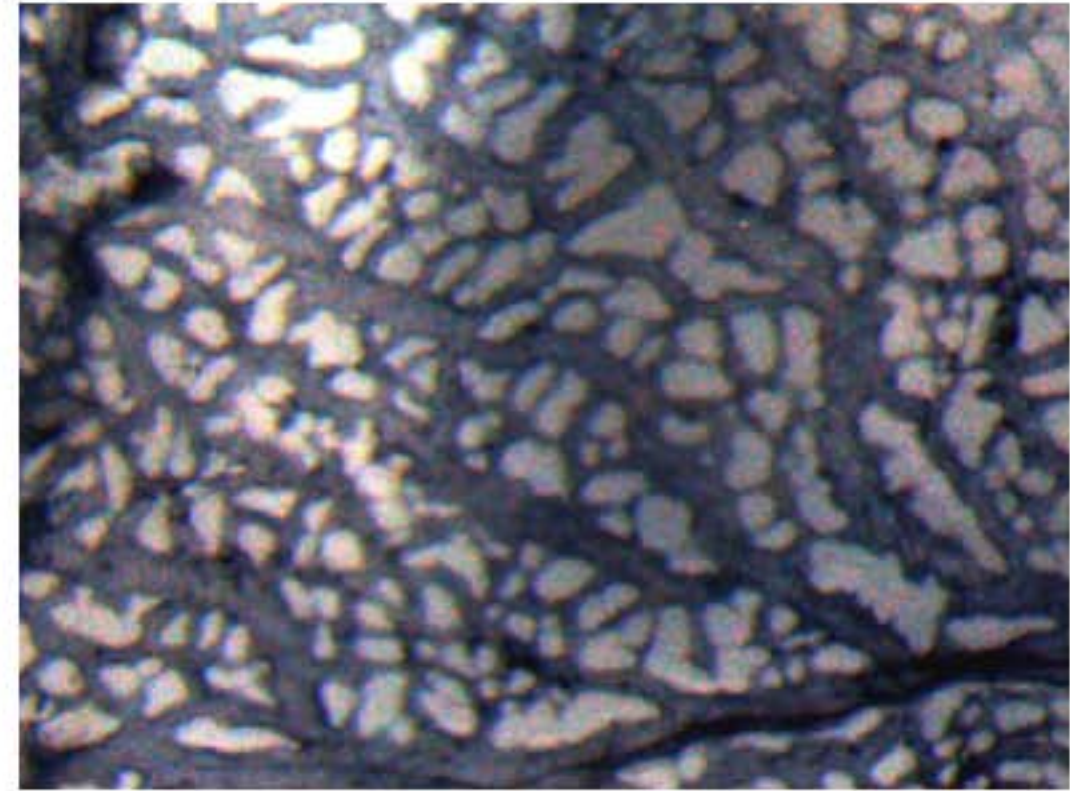
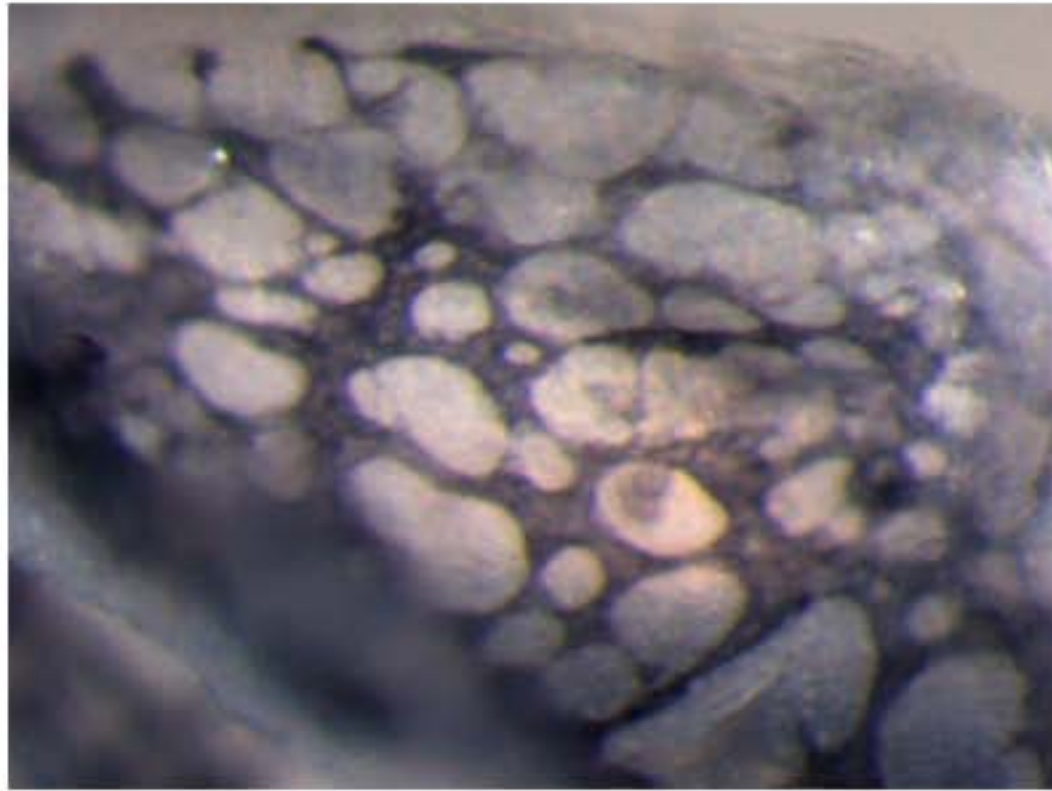




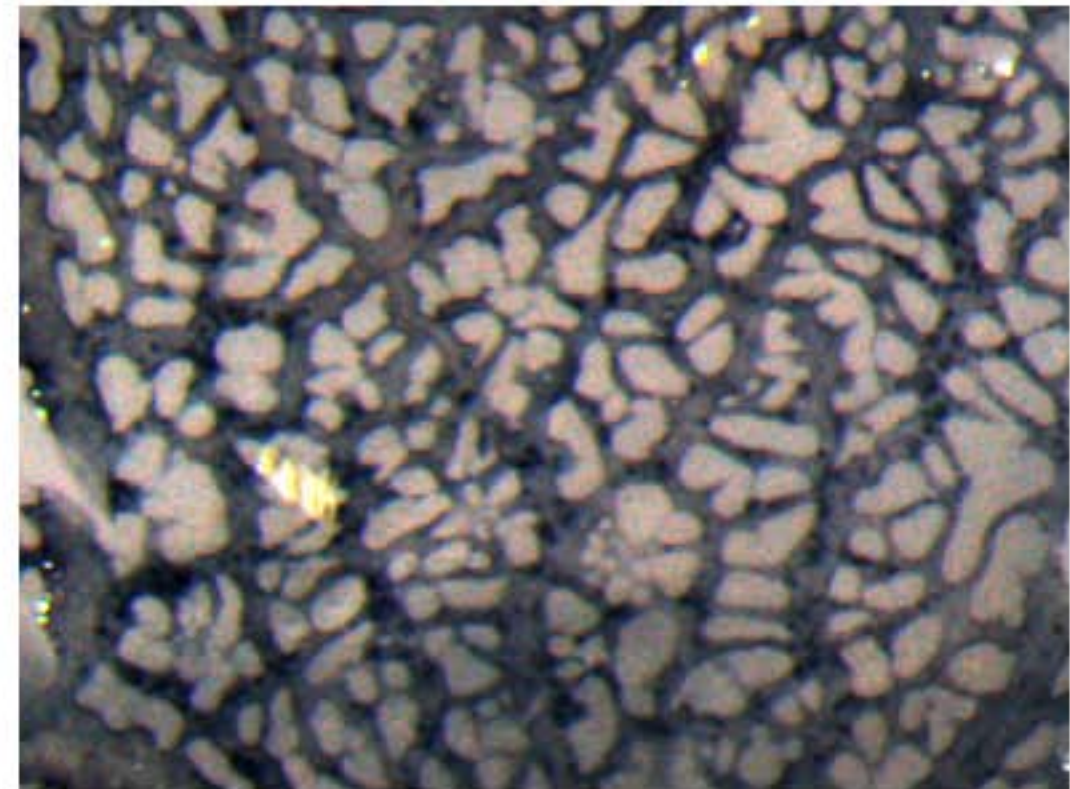
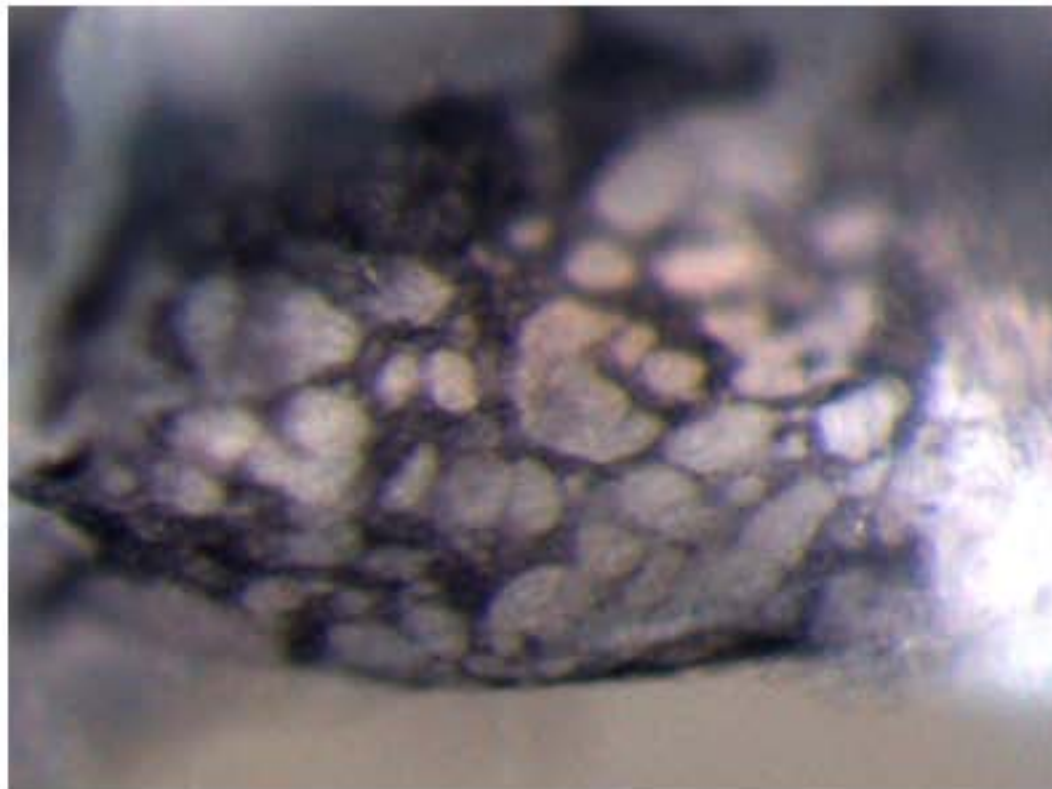
E8.5

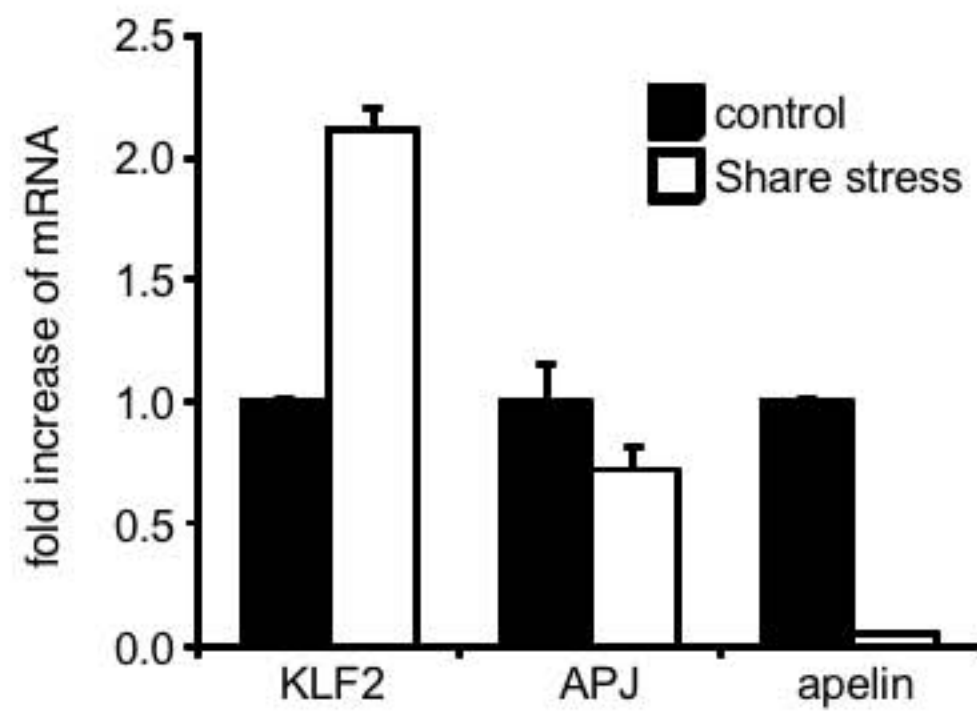
E9.5

WT

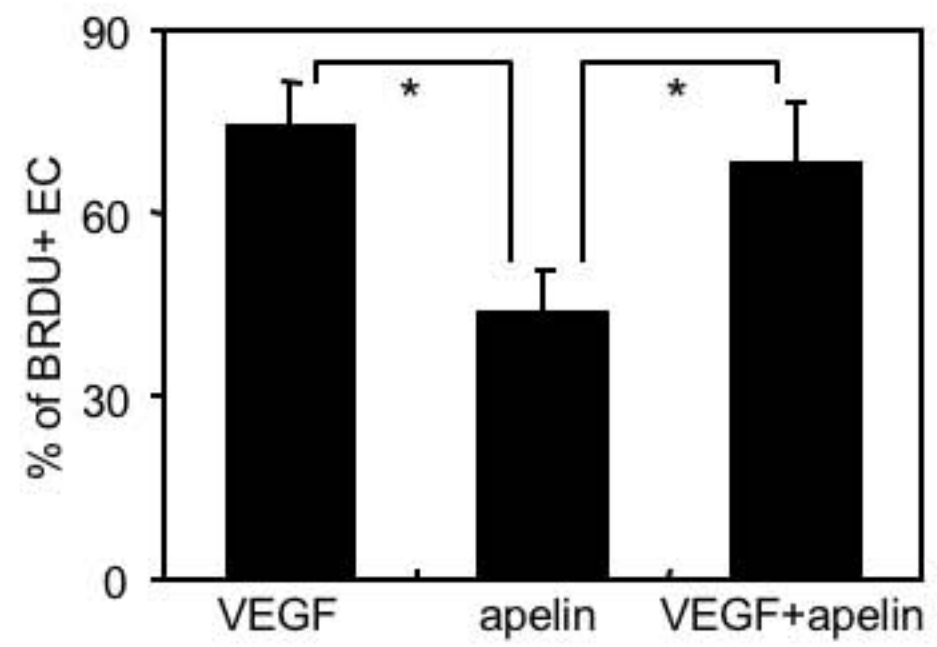


KO

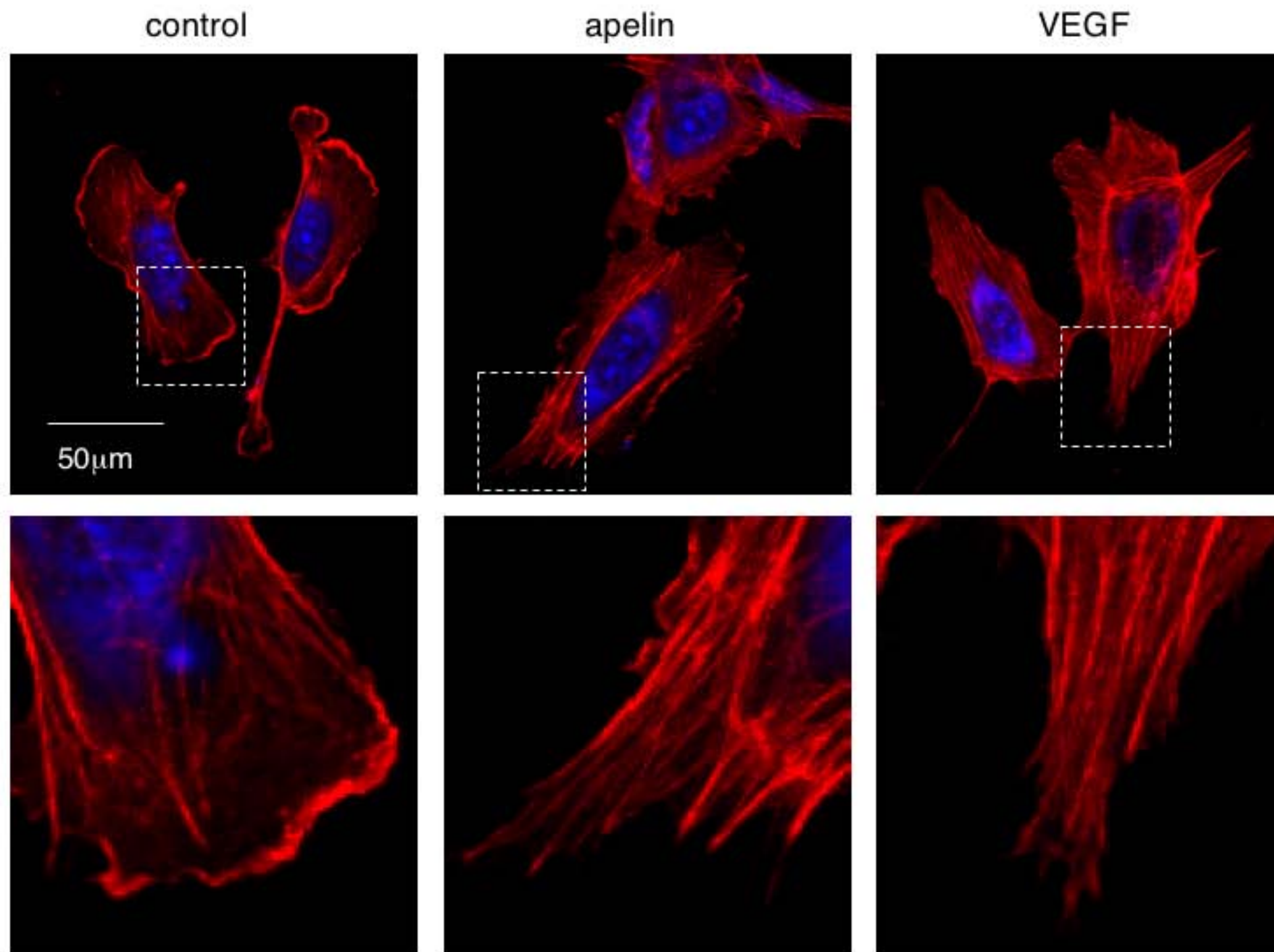




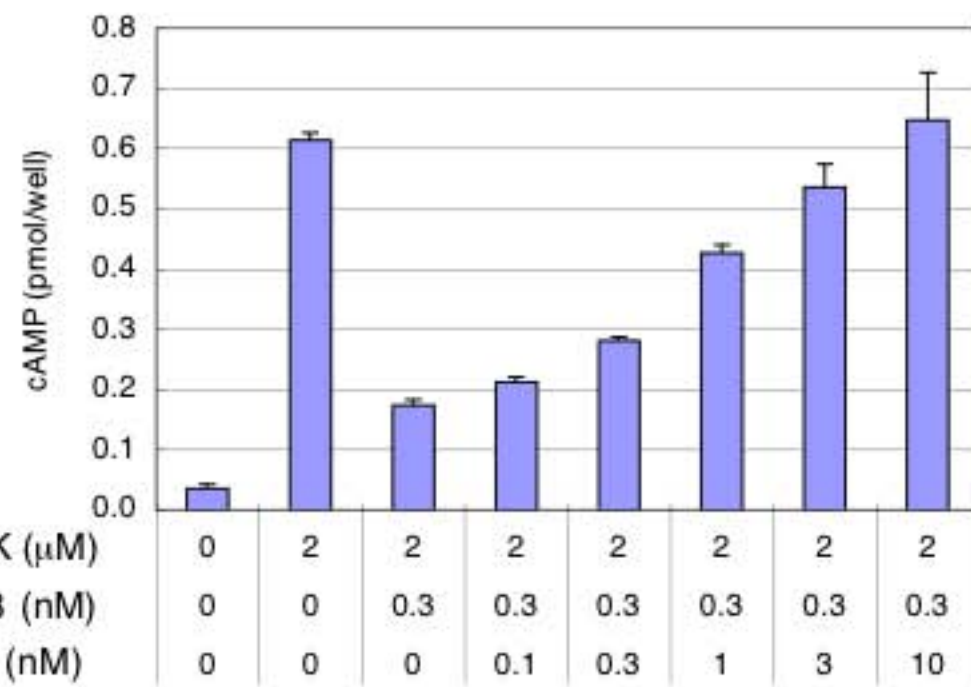
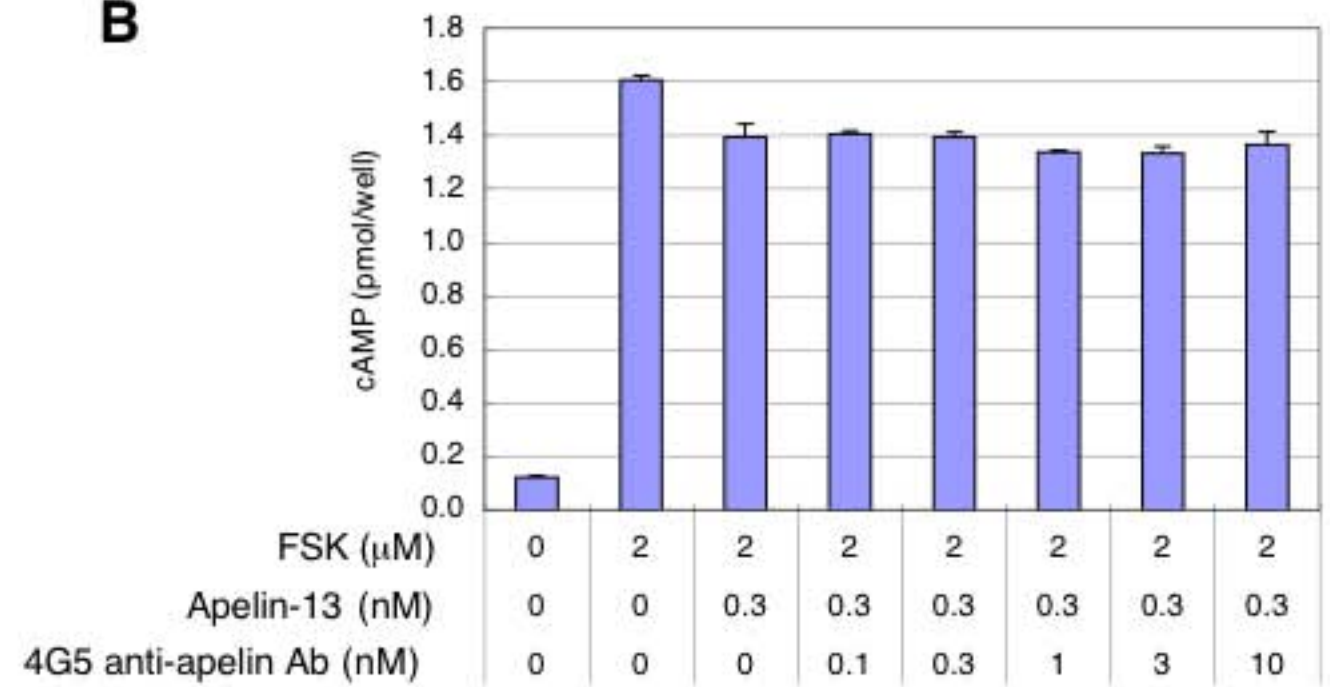
Supplementary Figure 13 Kidoya H. et al.



Supplementary Figure 14 Kidoya H. et al.



Supplemental Figure 15 Kidoya H. et al.

**A****B**

Supplementary Table 1 Oligonucleotide sequences for PCR

	Gene	Primer sequence	
Cloning and RT-PCR	<i>Mouse Apelin</i>	5'-GGAATTCGGGACCATGAATCTGAGGCTCTG-3'	
		5'-ACTTGGCGAGCCCTTCAATC-3	
Real-time PCR	<i>Mouse Apelin</i>		
	<i>Mouse APJ</i>	5'-GTGCCCTCCCGGTGCCGGTCTCT-3 5'-GAGACCACGCCATTAGAGGAACT-3	
	<i>Mouse GAPDH</i>	5'-CCACTGTGGGCCACTTATACC-3 5'-CAGCCTTAGCCGAGCATTG-3	
	<i>Human claudin5</i>	5'-TGGCAAAGTGGAGATTGTTGCC-3 5'-AAGATGGTGATGGGCTTCCCG-3	
	<i>Human VE-cadherin</i>	5'-TCGTTGCGCTCTTCGTGAC-3 5'-CAGCCCGCAAAACAGGTAG-3	
	<i>Human CD31</i>	5'-ATCGGTTGTTCAATGCGTCC-3 5'-CCTTCAGGATTTGGTACATGACA-3	
	<i>Human occludin</i>	5'-AACAGTGTTGACATGAAGAGCC-3 5'-TGTA AACAGCACGTCATCCTT-3	
	<i>Human GAPDH</i>	5'-CCCTTTTAGGAGGTAGTGTAGGC-3 5'-CCGTAGCCATAGCCATAACCA-3	
	RT-PCR	<i>Mouse APJ</i>	5'-GAAGGTGAAGGTCGGAGTC-3 5'-GAAGATGGTGATGGGATTTTC-3
			<i>Mouse GAPDH</i>